



Showcasing research from Qing-Fu Sun's laboratory, Fujian Institute of Research on the Structure of Matter, Fuzhou, China.

A self-assembled Pd<sub>2</sub>L<sub>4</sub> cage that selectively encapsulates nitrate

Inspiration of the artwork is from an Ancient Chinese Story, *i.e.*, 'Four Dragons Playing Bead' ('Si Long Xi Zhu' in Chinese). In this picture, the dragon represents the bidentate benzimidazole ligand, with an anthracene spacer. Four dragons twist (right- or left-handed, here right-handed) into a quadruple helicate conformation, defining a concise hydrophobic pocket. The ball represents the nitrate anion, which is selectively encapsulated inside.

As featured in:



See Li-Peng Zhou and Qing-Fu Sun, *Chem. Commun.*, 2015, **51**, 16767.

CrossMark  
click for updates

# A self-assembled Pd<sub>2</sub>L<sub>4</sub> cage that selectively encapsulates nitrate†

Li-Peng Zhou and Qing-Fu Sun\*

Cite this: *Chem. Commun.*, 2015, 51, 16767Received 31st August 2015,  
Accepted 28th September 2015

DOI: 10.1039/c5cc07306e

www.rsc.org/chemcomm

A M<sub>2</sub>L<sub>4</sub> cage with D<sub>4</sub> symmetry was self-assembled from four anthracene-bridged benzimidazole ligands and two Pd<sup>II</sup> ions. The cage features a concise hydrophobic pocket wrapped up by the anthracene walls with eight hydrogen-bond donors pointing inward, which provide a specific binding site for nitrate, with a binding affinity at least two orders of magnitude higher than all the other anions screened including halide anions, which have a very similar ionic radius and charge density.

Nitrate anion is ubiquitous and important in biology, the environment, and the food industry.<sup>1</sup> Although nitrate is probably benign, it can be reduced to nitrite or other nitric oxides, which react with thiols, amines and amides to form carcinogenic compounds. Other health concerns associated with NO<sub>3</sub><sup>-</sup> metabolism include diabetes, thyroid disorders, respiratory infections and congenital malformations.<sup>2,3</sup> Therefore, the design of a synthetic host with the capability of selective encapsulation of nitrate is an important task.

Many artificial hosts that can bind nitrate have been documented, including pyrrole,<sup>4,5</sup> amide,<sup>6–8</sup> ammonium,<sup>9,10</sup> urea,<sup>11</sup> guanidinium<sup>12</sup> based tripod,<sup>13</sup> macrocycle,<sup>14</sup> rotaxane,<sup>15</sup> catenane<sup>16</sup> or cage<sup>17</sup> like receptors. Because of the intrinsic properties of nitrate, the reported receptors have several common problems. First of all, large hydration energy and weak basicity of the nitrate anion result in that NO<sub>3</sub><sup>-</sup> is weakly coordinative and it is difficult to form robust hydrogen bonds with the host,<sup>2,17,18</sup> though hydrogen-bonding interaction plays a crucial role in the anion recognition process.<sup>19,20</sup> As a result, nitrate anion recognition has been mostly studied in less-polar solvents to favour the hydrogen bonding interactions, and in general poor binding affinity has been reported in polar solvents. Secondly, NO<sub>3</sub><sup>-</sup> has a D<sub>3h</sub> symmetry with equivalent N–O bonds. Based on the principle of geometrical matching,<sup>20</sup>

the hydrogen bond donors were limited to a complementary trigonal arrangement in the reported systems.<sup>15,21</sup> Thirdly, these receptors usually show limited selectivity for NO<sub>3</sub><sup>-</sup>.<sup>17</sup> Particularly, due to the negligible difference in ionic radii and charge densities between nitrate and halide anions, it is difficult to selectively recognize nitrate from halide anions.<sup>13,15</sup> Fourth, the most reported organic hosts generally require tedious multistep synthesis and in most cases give low yield. This means the design of a specific nitrate receptor is still very challenging.

The coordination cages,<sup>22–28</sup> readily self-assembled from simple organic ligand and metal components, have distinct advantages for the design of new ion receptors. Supramolecular organo-metallic cages avoid tedious synthesis; still they can be regulated easily *via* a rational symmetry consideration regarding the shape of the ligand, the coordination geometry of the metal, and the relative spatial orientation of the ligand and metal components. Although numerous coordination cages have been designed and synthesized for the encapsulation of anions in the literature,<sup>29–36</sup> to the best of our knowledge, an example where the differentiation between nitrate and halides by the host has never been reported due to the difficulties raised above.

Herein, we succeeded in designing a cationic M<sub>2</sub>L<sub>4</sub> cage by a quantitative self-assembly of four anthracene-bridged benzimidazole ligands and two Pd<sup>II</sup> ions (Fig. 1A). The cage showed a D<sub>4</sub> symmetry, but exhibited excellent capability in the selective encapsulation of nitrate. The binding constant (*K*<sub>anion</sub>) for the inclusion of NO<sub>3</sub><sup>-</sup> was at least two orders of magnitude higher than all the other anions screened.

Bidentate benzimidazole ligand **1**, with an anthracene spacer, was synthesized in two steps according to an established method.<sup>37</sup> After treating ligand **1** (18 μmol) with a half equivalent of Pd(NO<sub>3</sub>)<sub>2</sub> (9 μmol) in 700 μL *d*<sub>6</sub>-DMSO (dimethyl sulfoxide) for 2 h at 70 °C, the turbid solution turned limpid. The signals of the protons on the complex (**2a**) strongly split and shifted in comparison with those of the free ligand in the <sup>1</sup>H NMR spectrum (Fig. 1B and C). All the signals were assigned carefully based on coupling constants, integrals along with the correlations obtained from the <sup>1</sup>H–<sup>1</sup>H COSY spectrum (Fig. S5, ESI<sup>†</sup>). H<sub>a</sub> and H<sub>b</sub> of benzimidazole

State Key Laboratory of Structural Chemistry, Fujian Institute of Research on the Structure of Matter, Chinese Academy of Sciences, Fuzhou 350002, P. R. China.  
E-mail: qfsun@fjirsm.ac.cn; Fax: +86 591 63173527; Tel: +86 591 63173527

† Electronic supplementary information (ESI) available: Experimental details, supporting figures and tables. CCDC 1048711. For ESI and crystallographic data in CIF or other electronic format see DOI: 10.1039/c5cc07306e



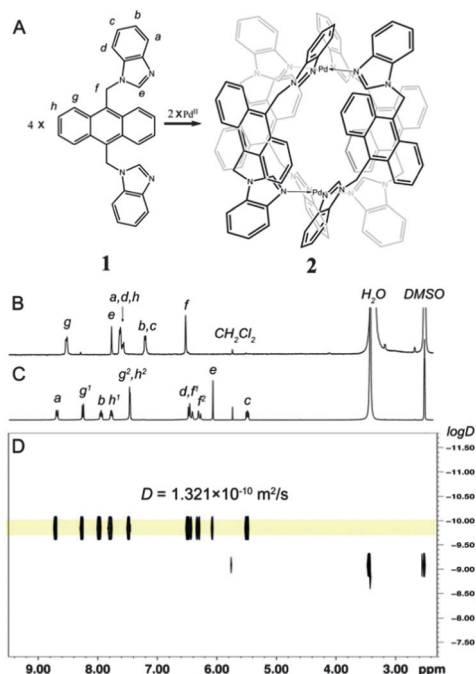


Fig. 1 (A) Self-assembly of complex **2**; the  $^1\text{H}$  NMR (400 MHz,  $d_6$ -DMSO, 298 K) spectrum of (B) ligand **1** and (C) complex **2a**; (D)  $^1\text{H}$  DOSY spectrum of complex **2a**.

were significantly shifted downfield (from 7.62 ppm and 7.21 ppm to 8.70 ppm and 7.95 ppm, respectively), which is diagnostic for the metal coordination. Diffusion-ordered NMR spectroscopy (DOSY) showed a single product with a single band at the diffusion coefficient  $D = 1.321 \times 10^{-10} \text{ m}^2 \text{ s}^{-1}$  ( $\log D = -9.879$ ) (Fig. 1D). The radius of the complex calculated from the  $D$  value was 8.42 Å, in accordance with the crystal structures of the complex (see discussion below).

Solid structural confirmation of **2a** was provided by X-ray crystallographic analysis. $\ddagger$  Suitable single crystals were obtained by slow diffusion of 1,4-dioxane vapour into a solution of **2a** in DMSO after about one week. Crystallographic data showed that four ligands in **2a** arranged in a quadruple helicate conformation due to the steric repulsion between the anthracene panels, resulting in a  $D_4$  symmetry of the host framework with inherent  $P$  or  $M$  helicity (Fig. 2A). Such helical chirality of the host must be maintained in solution to account for the observed diastereomeric splitting for proton  $\text{H}_{f,g,h}$  signals on the complex (Fig. 1C).

More interestingly, the four anthracene walls of the ligand wrap up a very concise hydrophobic cavity where all the benzimidazole protons are pointing inward, forming a perfect bind pocket that is occupied by a nitrate anion. Though the nitrate anion is in-plane disordered into four different orientations due to a mismatch of the symmetry, at each orientation its oxygen atoms are involved in at least six hydrogen bonding interactions with the benzimidazole  $\text{H}_e$  (Fig. 2B), with bonding distances of around 2.124–2.637 Å.

We happened to note that only three out of the four  $\text{NO}_3^-$  in **2a** could be replaced by  $\text{BF}_4^-$  after anion exchange by addition of an excess amount of  $\text{NaBF}_4$  in a typical anion exchange

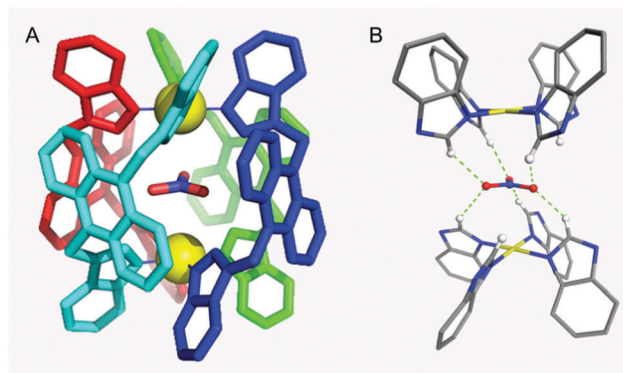


Fig. 2 (A) A perspective view of the crystal structure of **2a** with one encapsulated  $\text{NO}_3^-$  anion. (Note that the disorder of the central  $\text{NO}_3^-$  anion was not shown and four ligands were coloured differently to show the quadruple helicate conformation.) (B) Hydrogen bonding interactions (highlighted with green dashed lines) found between the  $\text{NO}_3^-$  and the benzimidazole ligands. All the other residual molecules were omitted for clarity.

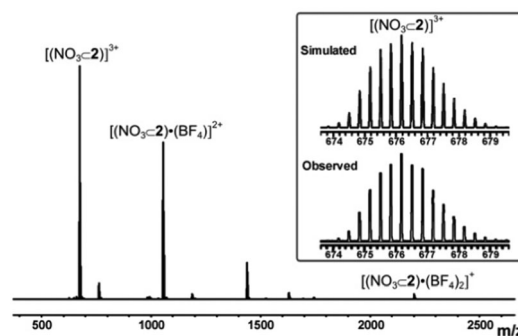


Fig. 3 ESI-Q-TOF mass spectrum of complex  $(\text{NO}_3 \subset 2) \cdot (\text{BF}_4)_3$ .

procedure, as revealed by ESI-Q-TOF mass spectroscopy (Fig. 3), which showed prominent peaks observed at  $m/z$  2202.5594, 1057.7774, 676.1837, corresponding to the  $[(\text{NO}_3 \subset 2) \cdot (\text{BF}_4)_{3-n}]^{n+}$ , ( $n = 1-3$ ) respectively. The finely resolved isotopic distribution at each MS signal was also in perfect agreement with the simulated pattern. The IR spectrum also confirmed that the nitrate occupied in the cavity of helicate (Fig. S8, ESI $\dagger$ ). This finding inspired us to estimate that cage **2** has a much stronger binding affinity for  $\text{NO}_3^-$  than  $\text{BF}_4^-$ .

When  $\text{Pd}(\text{CH}_3\text{CN})_4(\text{BF}_4)_2$  was used as the metal source,  $^1\text{H}$  and DOSY NMR spectra also suggested the quantitative formation of a similar metal-coordination cage (Fig. S9 and S12, ESI $\dagger$ ). However, the  $^1\text{H}$  NMR spectrum (complex **2b**) changed dramatically in comparison with that of **2a** (Fig. S23, ESI $\dagger$ ). This was the result of the encapsulation of  $\text{BF}_4^-$ , which was clearly confirmed by the  $^{19}\text{F}$  NMR spectrum (Fig. S11, ESI $\dagger$ ) and the ESI-Q-TOF mass spectrum (Fig. S14, ESI $\dagger$ ). In the  $^{19}\text{F}$  NMR spectrum, the signals corresponding to the encapsulated ( $-145.18$  ppm) and the free ( $-148.24$  ppm)  $\text{BF}_4^-$  anions were both observed. $^{30}$  When the bulkier guest  $\text{BF}_4^-$ , with a radius of 2.27 Å, $^{38}$  which is larger than  $\text{NO}_3^-$  (1.79 Å), was encapsulated *in situ* during the complexation, the cage had to adopt a more twisted configuration. So the difference of  $\delta_{\text{HF1}}$  with  $\delta_{\text{HF2}}$  increased, and  $\text{H}_b$  and  $\text{H}_c$  are more





downfield shifted. The difference in distortions was also suggested by the coordination conditions. It was necessary to prolong the reaction time or increase the temperature to 110 °C for the formation of **2b**, meaning that it had to overcome a higher energy barrier when  $\text{BF}_4^-$  was trapped into the cavity.

Though both  $\text{NO}_3^-$  and  $\text{BF}_4^-$  could be encapsulated, the cage showed distinct binding affinities between them. After treating **2b** with one equivalent of  $\text{KNO}_3$  at 110 °C, the  $^1\text{H}$  and  $^{19}\text{F}$  NMR spectrum revealed that **2b** converted to **2a** almost quantitatively with the encapsulated  $\text{BF}_4^-$  released (Fig. S24 and S25, ESI $^\dagger$ ), which confirmed that cage **2** bound  $\text{NO}_3^-$  more strongly than  $\text{BF}_4^-$ .

These observations urged us to make the empty cage **2** for further studies of its specific anion binding properties. We chose  $\text{Pd}(\text{PF}_6)_2$  (0.10 M solution in  $d_6$ -DMSO, prepared by reacting  $\text{PdCl}_2$  with  $\text{AgPF}_6$  in a 1:2 ratio at room temperature for 10 h under dark conditions, the  $\text{AgCl}$  precipitate was then removed by filtration) as the metal source. In contrast to  $\text{NO}_3^-$  and  $\text{BF}_4^-$ ,  $\text{PF}_6^-$  with an ionic radius of 2.54 Å<sup>38</sup> is significantly larger, and thus should not be encapsulated in the cavity. After treating ligand **1** with  $\text{Pd}(\text{PF}_6)_2$  for 2 h at 70 °C,  $^1\text{H}$  and DOSY NMR spectra all suggested the quantitative formation of a similar metal-coordination cage **2c** (Fig. S16 and S19, ESI $^\dagger$ ). The  $^{19}\text{F}$  NMR spectrum also confirmed that the  $\text{PF}_6^-$  was not encapsulated by the cage (Fig. S18, ESI $^\dagger$ ). However, the ESI-Q-TOF mass spectrum revealed that a chloride ion was trapped into the cavity (Fig. S21, ESI $^\dagger$ ). The contamination of  $\text{Cl}^-$  possibly comes from the preparation process of the  $\text{Pd}(\text{PF}_6)_2$  solution. This was also confirmed by the anion exchange reactions (Fig. S26 and S27, ESI $^\dagger$ ) by treating **2b** with 1.1 equivalent of  $\text{N}(\text{C}_4\text{H}_9)_4\text{Cl}$  at 110 °C, where new emerging signals attributed to **2c** were observed. The equilibrium constant, calculated by integrating the  $^1\text{H}$  NMR spectra, was around 40. The  $^{19}\text{F}$  NMR spectrum, showing that  $\text{BF}_4^-$  was replaced from the cavity by  $\text{Cl}^-$ , further proved the presence of  $\text{Cl}^-$  in **2c**.  $\text{Cl}^-$ , an ionic radius of 1.65 Å, is smaller than  $\text{NO}_3^-$  and  $\text{BF}_4^-$ , so **2c** twisted less. This was also supported by the  $^1\text{H}$  NMR spectrum, where a smaller diastereomeric splitting between  $\delta_{\text{Hf1}}$  with  $\delta_{\text{Hf2}}$  was observed in comparison to **2a** (Fig. S23, ESI $^\dagger$ ).

Nevertheless, the presence of  $\text{Cl}^-$  in the cavity of **2c** had no influence on the study of anion binding properties. Though the binding constants ( $K_{\text{anion}}$ ) could not be obtained, the relative binding ability (*versus*  $\text{Cl}^-$ ) could be exhibited. A series of anions available in the lab were screened for binding ability measurement by treating with cage **2c** (Fig. 4 and Fig. S28, ESI $^\dagger$ ), from which the equilibrium constants ( $K$ , *i.e.*,  $K_{\text{anion}}/K_{\text{Cl}}$ ) (Table 1) for the inclusion of anions, determined by the integration of the characteristic encapsulation signals in the  $^1\text{H}$  NMR experiments, were calculated.

For bulky anions, such as  $\text{CF}_3\text{SO}_3^-$ ,  $\text{H}_2\text{PO}_4^-$ , and  $\text{HSO}_4^-$ , no signals referenced to the anion-cage complex were observed. This probably was because they are too bulky to enter the cavity. For  $\text{Br}^-$ , the equilibrium constant was less than 1, meaning that the binding affinity is weaker than  $\text{Cl}^-$ . Presumably because the larger  $\text{Br}^-$  needs host **2** to keep a more high-energy twisted configuration, internal anions were exchanged. Similarly, but more obviously, less exchange for  $\text{BF}_4^-$  and  $\text{I}^-$  was observed because of their larger size. As for  $\text{F}^-$ , conversely, the smaller

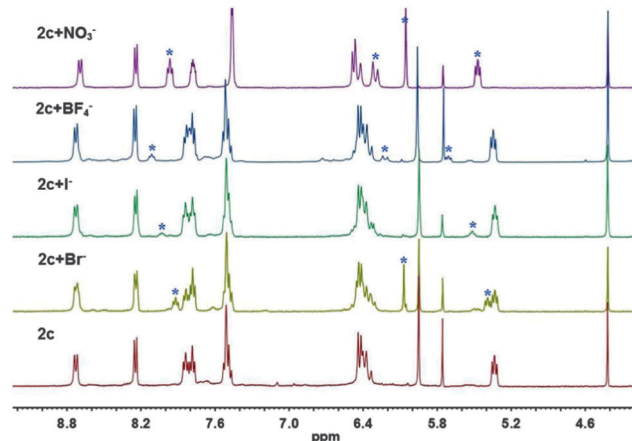


Fig. 4  $^1\text{H}$  NMR (400 MHz,  $d_6$ -DMSO, 298K) spectra showing the encapsulation of different anions by cage **2c**. (1.1 equivalent of anions were added to the solution of **2c** in  $d_6$ -DMSO, \* represents the new encapsulation signals.)

Table 1 The equilibrium constants<sup>a</sup> of anion exchange of **2c**

$\text{Cl}^- \subset \mathbf{2}(\mathbf{2c}) + \text{Anion} \xrightleftharpoons{K} \text{Anion} \subset \mathbf{2} + \text{Cl}^-$			
Anion	$K$	Anion	$K$
$\text{NO}_3^-$	$2.56 \times 10^2$	$\text{NO}_2^-$	$4.12 \times 10^{-3}$
$\text{Br}^-$	$2.86 \times 10^{-1}$	$\text{F}^-$	— <sup>c</sup>
$\text{I}^-$	$2.33 \times 10^{-2}$	$\text{Ac}^-$	— <sup>c</sup>
$\text{BF}_4^-$ <sup>b</sup>	$2.5 \times 10^{-2}$	$\text{CO}_3^{2-}$	— <sup>c</sup>

<sup>a</sup> Determined by the integration of the  $\text{H}_e$  signals except for the case of  $\text{BF}_4^-$  where the integration of  $\text{H}_c$  takes place because of signal overlapping. <sup>b</sup> Determined by the exchange of **2b** with  $\text{N}(\text{C}_4\text{H}_9)_4\text{Cl}$ . <sup>c</sup> No distinct exchange peaks appeared.

size made its spatial orientation inappropriate, so no distinct peaks appeared. The binding of cage **2** towards  $\text{Ac}^-$  and  $\text{CO}_3^{2-}$  was much weaker than  $\text{Cl}^-$  though they have similar size and geometry compared to nitrate anions.

Notably, for  $\text{NO}_3^-$ , the equilibrium constant was up to 256, in other words, cage **2** shows two orders of magnitude higher binding affinity toward  $\text{NO}_3^-$  than  $\text{Cl}^-$ . Moreover, in the kinetic experiments, the encapsulation of  $\text{NO}_3^-$  was faster than  $\text{Br}^-$  (Fig. S29–S31, ESI $^\dagger$ ). We attributed such a big difference to the presence of maximal hydrogen bonding interactions between the nitrate and the host cage in spite of the mismatching on symmetry. In contrast, the lack of hydrogen bonding weakens this binding between anions and the host even if their symmetries are better matching when single-atom halide anions were placed in the  $D_4$  symmetrical host. Similarly, little exchange for  $\text{NO}_2^-$  was observed.

In conclusion, a chiral  $\text{M}_2\text{L}_4$  cage was constructed from the coordination-driven self-assembly of the bidentate ligand **1** and  $\text{Pd}^{\text{II}}$  and showed distinct inclusion behaviour for different anions where unprecedented selective binding toward nitrate was observed.

This work was supported by the National Natural Science Foundation of China (Grant no. 21402201, 21471150, and 21221001), start-up foundation from FJIRSM-CAS, and award of “The Recruitment Program of Global Youth Experts”. We thank Prof. Da-Qiang Yuan (FJIRSM) for his kind assistance with the X-ray data collection.



## Notes and references

‡ Crystal data for **2a**: space group  $C_2$ ,  $a = 13.7980$  (14) Å,  $b = 32.546$  (4) Å,  $c = 13.7267$  (16) Å,  $\alpha = 90^\circ$ ,  $\beta = 100.330$  (10)°,  $\gamma = 90^\circ$ .  $V = 6064.3$  (12) Å<sup>3</sup>,  $Z = 2$ ,  $T = 102$  K.  $R_1 = 0.0971$ ,  $wR_2 = 0.2481$ , and goodness of fit = 1.075. CCDC 1048711.

- 1 B. Hay, D. Dixon, G. Lumetta, R. Vargas and J. Garza, in *Fundamentals and Applications of Anion Separations*, ed. B. Moyer and R. Singh, Springer, US2004, pp. 43–57.
- 2 M. Strianese, S. Millione, V. Bertolasi and C. Pellecchia, *Inorg. Chem.*, 2013, **52**, 11778–11786.
- 3 O. A. Okunola, P. V. Santacroce and J. T. Davis, *Supramol. Chem.*, 2008, **20**, 169–190.
- 4 J. L. Sessler, D. An, W.-S. Cho, V. Lynch and M. Marquez, *Chem. – Eur. J.*, 2005, **11**, 2001–2011.
- 5 J. L. Sessler, V. Roznyatovskiy, G. D. Pantos, N. E. Borisova, M. D. Reshetova, V. M. Lynch, V. N. Khrustalev and Y. A. Ustynyuk, *Org. Lett.*, 2005, **7**, 5277–5280.
- 6 A. P. Bisson, V. M. Lynch, M.-K. C. Monahan and E. V. Anslyn, *Angew. Chem., Int. Ed.*, 1997, **36**, 2340–2342.
- 7 J. M. Mahoney, K. A. Stucker, H. Jiang, I. Carmichael, N. R. Brinkmann, A. M. Beatty, B. C. Noll and B. D. Smith, *J. Am. Chem. Soc.*, 2005, **127**, 2922–2928.
- 8 B. Wu, J. Yang, X. Huang, S. Li, C. Jia, X.-J. Yang, N. Tang and C. Janiak, *Dalton Trans.*, 2011, **40**, 5687–5696.
- 9 S. Mason, T. Clifford, L. Seib, K. Kuczera and K. Bowman-James, *J. Am. Chem. Soc.*, 1998, **120**, 8899–8900.
- 10 L. Cronin, P. A. McGregor, S. Parsons, S. Teat, R. O. Gould, V. A. White, N. J. Long and N. Robertson, *Inorg. Chem.*, 2004, **43**, 8023–8029.
- 11 P. Byrne, G. O. Lloyd, N. Clarke and J. W. Steed, *Angew. Chem., Int. Ed.*, 2008, **47**, 5761–5764.
- 12 P. Blondeau, J. Benet-Buchholz and J. de Mendoza, *New J. Chem.*, 2007, **31**, 736–740.
- 13 M. Işıklan, M. A. Saeed, A. Pramanik, B. M. Wong, F. R. Fronczek and M. A. Hossain, *Cryst. Growth Des.*, 2011, **11**, 959–963.
- 14 R. Herges, A. Dikmans, U. Jana, F. Köhler, P. G. Jones, I. Dix, T. Fricke and B. König, *Eur. J. Org. Chem.*, 2002, 3004–3014.
- 15 M. J. Langton, L. C. Duckworth and P. D. Beer, *Chem. Commun.*, 2013, **49**, 8608–8610.
- 16 M. J. Langton and P. D. Beer, *Chem. Commun.*, 2014, **50**, 8124–8127.
- 17 J. Romański and P. Pitek, *J. Org. Chem.*, 2013, **78**, 4341–4347.
- 18 A. S. Singh and S.-S. Sun, *RSC Adv.*, 2012, **2**, 9502–9510.
- 19 K. Kavallieratos, C. M. Bertao and R. H. Crabtree, *J. Org. Chem.*, 1999, **64**, 1675–1683.
- 20 P. D. Beer and P. A. Gale, *Angew. Chem., Int. Ed.*, 2001, **40**, 486–516.
- 21 A. S. Singh and S.-S. Sun, *J. Org. Chem.*, 2012, **77**, 1880–1890.
- 22 S. M. Biroš, R. M. Yeh and K. N. Raymond, *Angew. Chem., Int. Ed.*, 2008, **47**, 6062–6064.
- 23 M. Yoshizawa, J. K. Klosterman and M. Fujita, *Angew. Chem., Int. Ed.*, 2009, **48**, 3418–3438.
- 24 G. H. Clever, S. Tashiro and M. Shionoya, *J. Am. Chem. Soc.*, 2010, **132**, 9973–9975.
- 25 M. Han, J. Hey, W. Kawamura, D. Stalke, M. Shionoya and G. H. Clever, *Inorg. Chem.*, 2012, **51**, 9574–9576.
- 26 J. J. Henkelis and M. J. Hardie, *Chem. Commun.*, 2015, **51**, 11929–11943.
- 27 N. J. Cookson, J. J. Henkelis, R. J. Ansell, C. W. G. Fishwick, M. J. Hardie and J. Fisher, *Dalton Trans.*, 2014, **43**, 5657–5661.
- 28 J. J. Henkelis, J. Fisher, S. L. Warriner and M. J. Hardie, *Chem. – Eur. J.*, 2014, **20**, 4117–4125.
- 29 R. Custelcean, *Chem. Soc. Rev.*, 2014, **43**, 1813–1824.
- 30 C. Klein, C. Gütz, M. Bogner, F. Topić, K. Rissanen and A. Lützen, *Angew. Chem., Int. Ed.*, 2014, **53**, 3739–3742.
- 31 H. Amouri, L. Mimassi, M. N. Rager, B. E. Mann, C. Guyard-Duhayon and L. Raehm, *Angew. Chem., Int. Ed.*, 2005, **44**, 4543–4546.
- 32 C. Desmarests, F. Poli, X. F. Le Goff, K. Muller and H. Amouri, *Dalton Trans.*, 2009, 10429–10432.
- 33 H. Amouri, C. Desmarests, A. Bettoschi, M. N. Rager, K. Boubekeur, P. Rabu and M. Drillon, *Chem. – Eur. J.*, 2007, **13**, 5401–5407.
- 34 S. Freye, R. Michel, D. Stalke, M. Pawliczek, H. Frauendorf and G. H. Clever, *J. Am. Chem. Soc.*, 2013, **135**, 8476–8479.
- 35 J. K. Clegg, J. Cremers, A. J. Hogben, B. Breiner, M. M. J. Smulders, J. D. Thoburn and J. R. Nitschke, *Chem. Sci.*, 2013, **4**, 68–76.
- 36 I. A. Riddell, M. M. J. Smulders, J. K. Clegg and J. R. Nitschke, *Chem. Commun.*, 2011, **47**, 457–459.
- 37 J.-L. Du, T.-L. Hu, S.-M. Zhang, Y.-F. Zeng and X.-H. Bu, *CrystEngComm*, 2008, **10**, 1866.
- 38 H. Tokuda, K. Hayamizu, K. Ishii, M. A. B. H. Susan and M. Watanabe, *J. Phys. Chem. B*, 2004, **108**, 16593–16600.

